

Measurement of the forward-backward asymmetries in the production of Ξ and Ω baryons in $p\bar{p}$ collisions

V.M. Abazov,³¹ B. Abbott,⁶⁷ B.S. Acharya,²⁵ M. Adams,⁴⁶ T. Adams,⁴⁴ J.P. Agnew,⁴¹ G.D. Alexeev,³¹ G. Alkhazov,³⁵ A. Alton^a,⁵⁶ A. Askew,⁴⁴ S. Atkins,⁵⁴ K. Augsten,⁷ V. Aushev,³⁸ Y. Aushev,³⁸ C. Avila,⁵ F. Badaud,¹⁰ L. Bagby,⁴⁵ B. Baldin,⁴⁵ D.V. Bandurin,⁷⁴ S. Banerjee,²⁵ E. Barberis,⁵⁵ P. Baringer,⁵³ J.F. Bartlett,⁴⁵ U. Bassler,¹⁵ V. Bazterra,⁴⁶ A. Bean,⁵³ M. Begalli,² L. Bellantoni,⁴⁵ S.B. Beri,²³ G. Bernardi,¹⁴ R. Bernhard,¹⁹ I. Bertram,³⁹ M. Besançon,¹⁵ R. Beuselinck,⁴⁰ P.C. Bhat,⁴⁵ S. Bhatia,⁵⁸ V. Bhatnagar,²³ G. Blazey,⁴⁷ S. Blessing,⁴⁴ K. Bloom,⁵⁹ A. Boehnlein,⁴⁵ D. Boline,⁶⁴ E.E. Boos,³³ G. Borissov,³⁹ M. Borysova^l,³⁸ A. Brandt,⁷¹ O. Brandt,²⁰ M. Brochmann,⁷⁵ R. Brock,⁵⁷ A. Bross,⁴⁵ D. Brown,¹⁴ X.B. Bu,⁴⁵ M. Buehler,⁴⁵ V. Buescher,²¹ V. Bunichev,³³ S. Burdin^b,³⁹ C.P. Buszello,³⁷ E. Camacho-Pérez,²⁸ B.C.K. Casey,⁴⁵ H. Castilla-Valdez,²⁸ S. Caughron,⁵⁷ S. Chakrabarti,⁶⁴ K.M. Chan,⁵¹ A. Chandra,⁷³ E. Chapon,¹⁵ G. Chen,⁵³ S.W. Cho,²⁷ S. Choi,²⁷ B. Choudhary,²⁴ S. Cihangir[†],⁴⁵ D. Claes,⁵⁹ J. Clutter,⁵³ M. Cooke^k,⁴⁵ W.E. Cooper,⁴⁵ M. Corcoran,⁷³ F. Couderc,¹⁵ M.-C. Cousinou,¹² J. Cuth,²¹ D. Cutts,⁷⁰ A. Das,⁷² G. Davies,⁴⁰ S.J. de Jong,^{29,30} E. De La Cruz-Burelo,²⁸ F. Déliot,¹⁵ R. Demina,⁶³ D. Denisov,⁴⁵ S.P. Denisov,³⁴ S. Desai,⁴⁵ C. Deterre^c,⁴¹ K. DeVaughan,⁵⁹ H.T. Diehl,⁴⁵ M. Diesburg,⁴⁵ P.F. Ding,⁴¹ A. Dominguez,⁵⁹ A. Dubey,²⁴ L.V. Dudko,³³ A. Duperrin,¹² S. Dutt,²³ M. Eads,⁴⁷ D. Edmunds,⁵⁷ J. Ellison,⁴³ V.D. Elvira,⁴⁵ Y. Enari,¹⁴ H. Evans,⁴⁹ A. Evdokimov,⁴⁶ V.N. Evdokimov,³⁴ A. Fauré,¹⁵ L. Feng,⁴⁷ T. Ferbel,⁶³ F. Fiedler,²¹ F. Filthaut,^{29,30} W. Fisher,⁵⁷ H.E. Fisk,⁴⁵ M. Fortner,⁴⁷ H. Fox,³⁹ J. Franc,⁷ S. Fuess,⁴⁵ P.H. Garbincius,⁴⁵ A. Garcia-Bellido,⁶³ J.A. García-González,²⁸ V. Gavrilov,³² W. Geng,^{12,57} C.E. Gerber,⁴⁶ Y. Gershtein,⁶⁰ G. Ginther,⁴⁵ O. Gogota,³⁸ G. Golovanov,³¹ P.D. Grannis,⁶⁴ S. Greder,¹⁶ H. Greenlee,⁴⁵ G. Grenier,¹⁷ Ph. Gris,¹⁰ J.-F. Grivaz,¹³ A. Grohsjean^c,¹⁵ S. Grünendahl,⁴⁵ M.W. Grünewald,²⁶ T. Guillemain,¹³ G. Gutierrez,⁴⁵ P. Gutierrez,⁶⁷ J. Haley,⁶⁸ L. Han,⁴ K. Harder,⁴¹ A. Harel,⁶³ J.M. Hauptman,⁵² J. Hays,⁴⁰ T. Head,⁴¹ T. Hebbeker,¹⁸ D. Hedin,⁴⁷ H. Hegab,⁶⁸ A.P. Heinson,⁴³ U. Heintz,⁷⁰ C. Hensel,¹ I. Heredia-De La Cruz^d,²⁸ K. Herner,⁴⁵ G. Hesketh^f,⁴¹ M.D. Hildreth,⁵¹ R. Hirosky,⁷⁴ T. Hoang,⁴⁴ J.D. Hobbs,⁶⁴ B. Hoeneisen,⁹ J. Hogan,⁷³ M. Hohlfeld,²¹ J.L. Holzbauer,⁵⁸ I. Howley,⁷¹ Z. Hubacek,^{7,15} V. Hynek,⁷ I. Iashvili,⁶² Y. Ilchenko,⁷² R. Illingworth,⁴⁵ A.S. Ito,⁴⁵ S. Jabeen^m,⁴⁵ M. Jaffré,¹³ A. Jayasinghe,⁶⁷ M.S. Jeong,²⁷ R. Jesik,⁴⁰ P. Jiang[†],⁴ K. Johns,⁴² E. Johnson,⁵⁷ M. Johnson,⁴⁵ A. Jonckheere,⁴⁵ P. Jonsson,⁴⁰ J. Joshi,⁴³ A.W. Jung^o,⁴⁵ A. Juste,³⁶ E. Kajfasz,¹² D. Karmanov,³³ I. Katsanos,⁵⁹ M. Kaur,²³ R. Kehoe,⁷² S. Kermiche,¹² N. Khalatyan,⁴⁵ A. Khanov,⁶⁸ A. Kharchilava,⁶² Y.N. Kharzheev,³¹ I. Kiselevich,³² J.M. Kohli,²³ A.V. Kozelov,³⁴ J. Kraus,⁵⁸ A. Kumar,⁶² A. Kupco,⁸ T. Kurča,¹⁷ V.A. Kuzmin,³³ S. Lammers,⁴⁹ P. Lebrun,¹⁷ H.S. Lee,²⁷ S.W. Lee,⁵² W.M. Lee,⁴⁵ X. Lei,⁴² J. Lellouch,¹⁴ D. Li,¹⁴ H. Li,⁷⁴ L. Li,⁴³ Q.Z. Li,⁴⁵ J.K. Lim,²⁷ D. Lincoln,⁴⁵ J. Linnemann,⁵⁷ V.V. Lipaev[†],³⁴ R. Lipton,⁴⁵ H. Liu,⁷² Y. Liu,⁴ A. Lobodenko,³⁵ M. Lokajicek,⁸ R. Lopes de Sa,⁴⁵ R. Luna-Garcia^g,²⁸ A.L. Lyon,⁴⁵ A.K.A. Maciel,¹ R. Madar,¹⁹ R. Magaña-Villalba,²⁸ S. Malik,⁵⁹ V.L. Malyshev,³¹ J. Mansour,²⁰ J. Martínez-Ortega,²⁸ R. McCarthy,⁶⁴ C.L. McGivern,⁴¹ M.M. Meijer,^{29,30} A. Melnitchouk,⁴⁵ D. Menezes,⁴⁷ P.G. Mercadante,³ M. Merkin,³³ A. Meyer,¹⁸ J. Meyerⁱ,²⁰ F. Miconi,¹⁶ N.K. Mondal,²⁵ M. Mulhearn,⁷⁴ E. Nagy,¹² M. Narain,⁷⁰ R. Nayyar,⁴² H.A. Neal,⁵⁶ J.P. Negret,⁵ P. Neustroev,³⁵ H.T. Nguyen,⁷⁴ T. Nunnemann,²² J. Orduna,⁷⁰ N. Osman,¹² A. Pal,⁷¹ N. Parashar,⁵⁰ V. Parihar,⁷⁰ S.K. Park,²⁷ R. Partridge^e,⁷⁰ N. Parua,⁴⁹ A. Patwa^j,⁶⁵ B. Penning,⁴⁰ M. Perfilov,³³ Y. Peters,⁴¹ K. Petridis,⁴¹ G. Petrillo,⁶³ P. Pétroff,¹³ M.-A. Pleier,⁶⁵ V.M. Podstavkov,⁴⁵ A.V. Popov,³⁴ M. Prewitt,⁷³ D. Price,⁴¹ N. Prokopenko,³⁴ J. Qian,⁵⁶ A. Quadt,²⁰ B. Quinn,⁵⁸ P.N. Ratoff,³⁹ I. Razumov,³⁴ I. Ripp-Baudot,¹⁶ F. Rizatdinova,⁶⁸ M. Rominsky,⁴⁵ A. Ross,³⁹ C. Royon,⁸ P. Rubinov,⁴⁵ R. Ruchti,⁵¹ G. Sajot,¹¹ A. Sánchez-Hernández,²⁸ M.P. Sanders,²² A.S. Santos^h,¹ G. Savage,⁴⁵ M. Savitskyi,³⁸ L. Sawyer,⁵⁴ T. Scanlon,⁴⁰ R.D. Schamberger,⁶⁴ Y. Scheglov,³⁵ H. Schellman,^{69,48} M. Schott,²¹ C. Schwanenberger,⁴¹ R. Schwienhorst,⁵⁷ J. Sekaric,⁵³ H. Severini,⁶⁷ E. Shabalina,²⁰ V. Shary,¹⁵ S. Shaw,⁴¹ A.A. Shchukin,³⁴ V. Simak,⁷ P. Skubic,⁶⁷ P. Slattery,⁶³ G.R. Snow,⁵⁹ J. Snow,⁶⁶ S. Snyder,⁶⁵ S. Söldner-Rembold,⁴¹ L. Sonnenschein,¹⁸ K. Soustruznik,⁶ J. Stark,¹¹ N. Stefaniuk,³⁸ D.A. Stoyanova,³⁴ M. Strauss,⁶⁷ L. Suter,⁴¹ P. Svoisky,⁷⁴ M. Titov,¹⁵ V.V. Tokmenin,³¹ Y.-T. Tsai,⁶³ D. Tsybychev,⁶⁴ B. Tuchming,¹⁵ C. Tully,⁶¹ L. Uvarov,³⁵ S. Uvarov,³⁵ S. Uzunyan,⁴⁷ R. Van Kooten,⁴⁹ W.M. van Leeuwen,²⁹ N. Varelas,⁴⁶ E.W. Varnes,⁴² I.A. Vasilyev,³⁴ A.Y. Verkheev,³¹ L.S. Vertogradov,³¹ M. Verzocchi,⁴⁵ M. Vesterinen,⁴¹

D. Vilanova,¹⁵ P. Vokac,⁷ H.D. Wahl,⁴⁴ M.H.L.S. Wang,⁴⁵ J. Warchol,⁵¹ G. Watts,⁷⁵ M. Wayne,⁵¹ J. Weichert,²¹ L. Welty-Rieger,⁴⁸ M.R.J. Williamsⁿ,⁴⁹ G.W. Wilson,⁵³ M. Wobisch,⁵⁴ D.R. Wood,⁵⁵ T.R. Wyatt,⁴¹ Y. Xie,⁴⁵ R. Yamada,⁴⁵ S. Yang,⁴ T. Yasuda,⁴⁵ Y.A. Yatsunenko,³¹ W. Ye,⁶⁴ Z. Ye,⁴⁵ H. Yin,⁴⁵ K. Yip,⁶⁵ S.W. Youn,⁴⁵ J.M. Yu,⁵⁶ J. Zennamo,⁶² T.G. Zhao,⁴¹ B. Zhou,⁵⁶ J. Zhu,⁵⁶ M. Zielinski,⁶³ D. Zieminska,⁴⁹ and L. Zivkovic¹⁴

(The D0 Collaboration*)

¹LAFEX, Centro Brasileiro de Pesquisas Físicas, Rio de Janeiro, RJ 22290, Brazil

²Universidade do Estado do Rio de Janeiro, Rio de Janeiro, RJ 20550, Brazil

³Universidade Federal do ABC, Santo André, SP 09210, Brazil

⁴University of Science and Technology of China, Hefei 230026, People's Republic of China

⁵Universidad de los Andes, Bogotá, 111711, Colombia

⁶Charles University, Faculty of Mathematics and Physics,

Center for Particle Physics, 116 36 Prague 1, Czech Republic

⁷Czech Technical University in Prague, 116 36 Prague 6, Czech Republic

⁸Institute of Physics, Academy of Sciences of the Czech Republic, 182 21 Prague, Czech Republic

⁹Universidad San Francisco de Quito, Quito, Ecuador

¹⁰LPC, Université Blaise Pascal, CNRS/IN2P3, Clermont, F-63178 Aubière Cedex, France

¹¹LPSC, Université Joseph Fourier Grenoble 1, CNRS/IN2P3,

Institut National Polytechnique de Grenoble, F-38026 Grenoble Cedex, France

¹²CPPM, Aix-Marseille Université, CNRS/IN2P3, F-13288 Marseille Cedex 09, France

¹³LAL, Univ. Paris-Sud, CNRS/IN2P3, Université Paris-Saclay, F-91898 Orsay Cedex, France

¹⁴LPNHE, Universités Paris VI and VII, CNRS/IN2P3, F-75005 Paris, France

¹⁵CEA Saclay, Irfu, SPP, F-91191 Gif-Sur-Yvette Cedex, France

¹⁶IPHC, Université de Strasbourg, CNRS/IN2P3, F-67037 Strasbourg, France

¹⁷IPNL, Université Lyon 1, CNRS/IN2P3, F-69622 Villeurbanne Cedex,

France and Université de Lyon, F-69361 Lyon CEDEX 07, France

¹⁸III. Physikalisches Institut A, RWTH Aachen University, 52056 Aachen, Germany

¹⁹Physikalisches Institut, Universität Freiburg, 79085 Freiburg, Germany

²⁰II. Physikalisches Institut, Georg-August-Universität Göttingen, 37073 Göttingen, Germany

²¹Institut für Physik, Universität Mainz, 55099 Mainz, Germany

²²Ludwig-Maximilians-Universität München, 80539 München, Germany

²³Panjab University, Chandigarh 160014, India

²⁴Delhi University, Delhi-110 007, India

²⁵Tata Institute of Fundamental Research, Mumbai-400 005, India

²⁶University College Dublin, Dublin 4, Ireland

²⁷Korea Detector Laboratory, Korea University, Seoul, 02841, Korea

²⁸CINVESTAV, Mexico City 07360, Mexico

²⁹Nikhef, Science Park, 1098 XG Amsterdam, the Netherlands

³⁰Radboud University Nijmegen, 6525 AJ Nijmegen, the Netherlands

³¹Joint Institute for Nuclear Research, Dubna 141980, Russia

³²Institute for Theoretical and Experimental Physics, Moscow 117259, Russia

³³Moscow State University, Moscow 119991, Russia

³⁴Institute for High Energy Physics, Protvino, Moscow region 142281, Russia

³⁵Petersburg Nuclear Physics Institute, St. Petersburg 188300, Russia

³⁶Institució Catalana de Recerca i Estudis Avançats (ICREA) and Institut de Física d'Altes Energies (IFAE), 08193 Bellaterra (Barcelona), Spain

³⁷Uppsala University, 751 05 Uppsala, Sweden

³⁸Taras Shevchenko National University of Kyiv, Kiev, 01601, Ukraine

³⁹Lancaster University, Lancaster LA1 4YB, United Kingdom

⁴⁰Imperial College London, London SW7 2AZ, United Kingdom

⁴¹The University of Manchester, Manchester M13 9PL, United Kingdom

⁴²University of Arizona, Tucson, Arizona 85721, USA

⁴³University of California Riverside, Riverside, California 92521, USA

⁴⁴Florida State University, Tallahassee, Florida 32306, USA

⁴⁵Fermi National Accelerator Laboratory, Batavia, Illinois 60510, USA

⁴⁶University of Illinois at Chicago, Chicago, Illinois 60607, USA

⁴⁷Northern Illinois University, DeKalb, Illinois 60115, USA

⁴⁸Northwestern University, Evanston, Illinois 60208, USA

⁴⁹Indiana University, Bloomington, Indiana 47405, USA

⁵⁰Purdue University Calumet, Hammond, Indiana 46323, USA

⁵¹University of Notre Dame, Notre Dame, Indiana 46556, USA

⁵²Iowa State University, Ames, Iowa 50011, USA

⁵³University of Kansas, Lawrence, Kansas 66045, USA

- ⁵⁴Louisiana Tech University, Ruston, Louisiana 71272, USA
⁵⁵Northeastern University, Boston, Massachusetts 02115, USA
⁵⁶University of Michigan, Ann Arbor, Michigan 48109, USA
⁵⁷Michigan State University, East Lansing, Michigan 48824, USA
⁵⁸University of Mississippi, University, Mississippi 38677, USA
⁵⁹University of Nebraska, Lincoln, Nebraska 68588, USA
⁶⁰Rutgers University, Piscataway, New Jersey 08855, USA
⁶¹Princeton University, Princeton, New Jersey 08544, USA
⁶²State University of New York, Buffalo, New York 14260, USA
⁶³University of Rochester, Rochester, New York 14627, USA
⁶⁴State University of New York, Stony Brook, New York 11794, USA
⁶⁵Brookhaven National Laboratory, Upton, New York 11973, USA
⁶⁶Langston University, Langston, Oklahoma 73050, USA
⁶⁷University of Oklahoma, Norman, Oklahoma 73019, USA
⁶⁸Oklahoma State University, Stillwater, Oklahoma 74078, USA
⁶⁹Oregon State University, Corvallis, Oregon 97331, USA
⁷⁰Brown University, Providence, Rhode Island 02912, USA
⁷¹University of Texas, Arlington, Texas 76019, USA
⁷²Southern Methodist University, Dallas, Texas 75275, USA
⁷³Rice University, Houston, Texas 77005, USA
⁷⁴University of Virginia, Charlottesville, Virginia 22904, USA
⁷⁵University of Washington, Seattle, Washington 98195, USA
- (Dated: May 11, 2016)

We measure the forward-backward asymmetries A_{FB} of charged Ξ and Ω baryons produced in $p\bar{p}$ collisions recorded by the D0 detector at the Fermilab Tevatron collider at $\sqrt{s} = 1.96$ TeV as a function of the baryon rapidity y . We find that the asymmetries A_{FB} for charged Ξ and Ω baryons are consistent with zero within statistical uncertainties.

INTRODUCTION

We present a study of the forward-backward asymmetries A_{FB} for the production of charged Ξ and Ω baryons in $p\bar{p}$ collisions at a center of mass energy $\sqrt{s} = 1.96$ TeV, recorded by the D0 detector at the Fermilab Tevatron collider.

We previously performed a study of A_{FB} for Λ and $\bar{\Lambda}$ production [1], where A_{FB} is defined as the relative excess of Λ ($\bar{\Lambda}$) baryons produced with longitudinal momentum p_z in the p (\bar{p}) direction. These results are in agreement with the observations in a wide range of proton collision experiments that the $\bar{\Lambda}/\Lambda$ production ratio follows a universal function of the ‘‘rapidity loss’’ $y_p - y$ between

the beam proton and the produced $\bar{\Lambda}$ or Λ baryon which does not depend significantly on \sqrt{s} or on the nature of the target p , \bar{p} , Be, or Pb (see Ref. [1] and references therein). These results support the view that a strange quark produced directly in the hard scattering of point-like partons, or indirectly in the subsequent showering, can coalesce with a diquark remnant of the beam particle to produce a Λ baryon with a probability that increases as the rapidity difference between the incoming proton and outgoing Λ baryon decreases.

If this hypothesis is correct, we also expect $A_{FB} > 0$ for Λ_c ($\bar{\Lambda}_c$), and Λ_b ($\bar{\Lambda}_b$) production in which a c or b quark can coalesce with a diquark from the proton. For the B mesons and Ξ and Ω baryons, we expect $A_{FB} \approx 0$ since these particles do not share a diquark with the proton. Previous D0 measurements include $A_{FB}(B^-, B^+)$ [2] and $A_{FB}(\Lambda_b, \bar{\Lambda}_b)$ [3].

In this article, we present measurements of the forward-backward asymmetries of Ξ^\mp and Ω^\mp production, where we use the notation $\Xi^+ \equiv \bar{\Xi}^-$ and $\Omega^+ \equiv \bar{\Omega}^-$. The Ξ^- and Ξ^+ baryons are defined as ‘‘forward’’ if their p_z points in the p or \bar{p} direction, respectively. The asymmetry A_{FB} is defined as

$$A_{FB} \equiv \frac{\sigma_F(\Xi^-) - \sigma_B(\Xi^-) + \sigma_F(\Xi^+) - \sigma_B(\Xi^+)}{\sigma_F(\Xi^-) + \sigma_B(\Xi^-) + \sigma_F(\Xi^+) + \sigma_B(\Xi^+)}, \quad (1)$$

where σ_F and σ_B are the forward and backward cross sections of Ξ^- or Ξ^+ production, and similarly for Ω^\mp baryons. The measurements include Ξ^\mp and Ω^\mp baryons that are either directly produced or decay products of

*with visitors from ^aAugustana College, Sioux Falls, SD 57197, USA, ^bThe University of Liverpool, Liverpool L69 3BX, UK, ^cDeutsches Elektronen-Synchrotron (DESY), Notkestrasse 85, Germany, ^dCONACyT, M-03940 Mexico City, Mexico, ^eSLAC, Menlo Park, CA 94025, USA, ^fUniversity College London, London WC1E 6BT, UK, ^gCentro de Investigacion en Computacion - IPN, CP 07738 Mexico City, Mexico, ^hUniversidade Estadual Paulista, São Paulo, SP 01140, Brazil, ⁱKarlsruher Institut für Technologie (KIT) - Steinbuch Centre for Computing (SCC), D-76128 Karlsruhe, Germany, ^jOffice of Science, U.S. Department of Energy, Washington, D.C. 20585, USA, ^kAmerican Association for the Advancement of Science, Washington, D.C. 20005, USA, ^lKiev Institute for Nuclear Research (KINR), Kyiv 03680, Ukraine, ^mUniversity of Maryland, College Park, MD 20742, USA, ⁿEuropean Organization for Nuclear Research (CERN), CH-1211 Geneva, Switzerland and ^oPurdue University, West Lafayette, IN 47907, USA. [‡]Deceased.

heavier hadrons. The measurement strategy for the asymmetry A_{FB} of Ξ^\mp and Ω^\mp baryons presented here closely follows the analysis method used to determine A_{FB} for Λ and $\bar{\Lambda}$ baryons in Ref. [1].

DETECTOR AND DATA

The D0 detector is described in detail in Refs. [4–7]. The collision region is surrounded by a central tracking system that comprises a silicon microstrip vertex detector and a central fiber tracker, both located within a 1.9 T superconducting solenoidal magnet [4], surrounded successively by the liquid-argon/uranium calorimeters, a layer of the muon system [5], comprising drift chambers and scintillation trigger counters, the 1.8 T magnetized iron toroids, and two additional muon detector layers after the toroids.

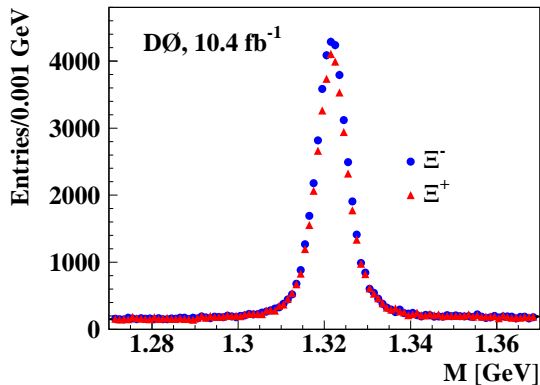


FIG. 1: Invariant mass distributions of reconstructed $\Xi^- \rightarrow \Lambda\pi^-$ (circles) and $\Xi^+ \rightarrow \bar{\Lambda}\pi^+$ (triangles) for $p\bar{p} \rightarrow \mu\Xi^\mp X$ data.

The longitudinal momentum p_z and the rapidity $y \equiv \ln[(E + p_z)/(E - p_z)]/2$ are both measured with respect to the proton beam direction in the $p\bar{p}$ center of mass frame where E is the energy of the baryon. We present results for the full integrated luminosity of 10.4 fb^{-1} , collected from 2002 to 2011, using two data sets (i) $p\bar{p} \rightarrow \Xi^\mp X$, and (ii) $p\bar{p} \rightarrow \mu\Xi^\mp X$. The first data set is unbiased since it is collected using a pre-scaled trigger on beam crossing (“zero bias events”) or with a pre-scaled trigger on energy deposited in the forward counters (“minimum bias events”). The second data set is selected with a suite of single muon triggers which implies that most events contain heavy-quark (b or c) decays. This data set is defined using the same muon triggers and muon selections as in Ref. [8, 9]. The muon data provides a sizable data set that adds additional statistics for the analysis. For Ω ’s there are fewer events, so we only present results for the set $p\bar{p} \rightarrow \mu\Omega^\mp X$.

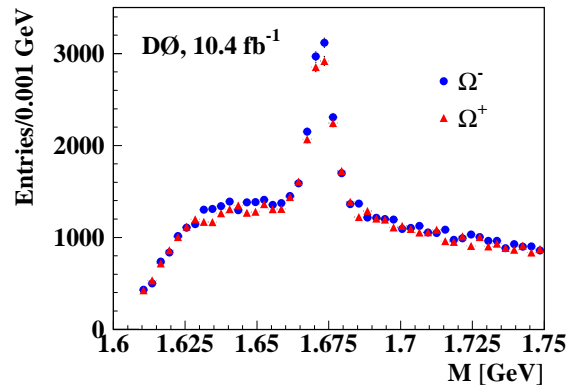


FIG. 2: Invariant mass distributions of reconstructed $\Omega^- \rightarrow \Lambda K^-$ (circles) and $\Omega^+ \rightarrow \bar{\Lambda} K^+$ (triangles) for $p\bar{p} \rightarrow \mu\Omega^\mp X$ data.

We observe Ξ baryons through their decays $\Xi^- \rightarrow \Lambda\pi^-$ and $\Xi^+ \rightarrow \bar{\Lambda}\pi^+$, and Ω baryons through their decays $\Omega^- \rightarrow \Lambda K^-$ and $\Omega^+ \rightarrow \bar{\Lambda} K^+$, with $\Lambda \rightarrow p\pi^-$ and $\bar{\Lambda} \rightarrow \bar{p}\pi^+$ in both cases. The Λ and $\bar{\Lambda}$ candidates are reconstructed from pairs of oppositely curved tracks with a common vertex (V^0). Each track is required to have a non-zero impact parameter in the transverse plane (IP) with respect to the $p\bar{p}$ interaction vertex with a significance of at least two standard deviations. The proton (pion) mass is assigned to the daughter track with larger (smaller) total momentum since the decay $\Lambda \rightarrow p\pi$ is just above threshold. The invariant mass of the (p, π^-) or (\bar{p}, π^+) pair is required to be in the interval $1.105 < M(p\pi) < 1.125 \text{ GeV}$ [1]. We require Λ and $\bar{\Lambda}$ candidates with $1.5 < p_T < 25 \text{ GeV}$ and pseudorapidity $|\eta| < 2.2$ [10], and their IP must be non-zero with a significance greater than two standard deviations.

The Λ ($\bar{\Lambda}$) candidate is combined with a negatively (positively) charged-particle track with separation in the transverse plane from the primary vertex with significance greater than three standard deviations and a good vertex with the Λ ($\bar{\Lambda}$) candidate. This track is assigned the pion mass for Ξ ’s or the kaon mass for Ω ’s. The Ξ^\mp or Ω^\mp candidates are required to have an IP consistent with zero within three standard deviations. The observed decay lengths in the transverse plane of the Λ and Ξ^- or Ω^- (or $\bar{\Lambda}$ and Ξ^+ or Ω^+) are required to be greater than 4 mm. The invariant mass for the Ξ^\mp candidate is required to be in the interval $1.2 < M(\Lambda\pi) < 1.5 \text{ GeV}$ and $1.55 < M(\Lambda K) < 1.85 \text{ GeV}$ for Ω^\mp candidates. The kinematic selections for the Ξ^\mp and Ω^\mp candidates are $p_T > 2.0 \text{ GeV}$ and $|\eta| < 2.2$. The pion or kaon track and the two daughter tracks of the Λ baryon are required to be different from any track associated to a muon. The invariant mass distributions for the decays $\Xi^- \rightarrow \Lambda\pi^-$ and $\Xi^+ \rightarrow \bar{\Lambda}\pi^+$ are shown in Fig. 1 and for the decays

$\Omega^- \rightarrow \Lambda K^-$ and $\Omega^+ \rightarrow \bar{\Lambda} K^+$ in Fig. 2.

RAW ASYMMETRIES AND DETECTOR EFFECTS

We obtain the numbers $N_F(\Xi^\mp)$ and $N_B(\Xi^\mp)$ of reconstructed Ξ^\mp baryons in the forward and backward categories in each bin of $|y|$ by counting Ξ^\mp candidates in the signal region, $1.305 < M(\Lambda\pi) < 1.335$ GeV, and subtracting the counts in two sideband regions, defined by $1.2775 < M(\Lambda\pi) < 1.2925$ GeV and $1.3475 < M(\Lambda\pi) < 1.3625$ GeV. The signal region for Ω^\mp candidates is $1.6575 < M(\Lambda K) < 1.6875$ GeV, and the sideband regions are $1.630 < M(\Lambda K) < 1.645$ GeV and $1.700 < M(\Lambda K) < 1.715$ GeV.

The normalization factor N and the three raw asymmetries A'_{FB} , A'_{NS} , and A'_Ξ are defined by

$$\begin{aligned} N_F(\Xi^-) &\equiv N(1 + A'_{\text{FB}})(1 - A'_{\text{NS}})(1 + A'_\Xi), \\ N_B(\Xi^-) &\equiv N(1 - A'_{\text{FB}})(1 + A'_{\text{NS}})(1 + A'_\Xi), \\ N_F(\Xi^+) &\equiv N(1 + A'_{\text{FB}})(1 + A'_{\text{NS}})(1 - A'_\Xi), \\ N_B(\Xi^+) &\equiv N(1 - A'_{\text{FB}})(1 - A'_{\text{NS}})(1 - A'_\Xi), \end{aligned} \quad (2)$$

and similarly for Ω . The raw asymmetries A'_{FB} , A'_{NS} , and A'_Ξ have contributions from the physical asymmetries A_{FB} , A_{NS} , and A_Ξ , and from detector effects. The forward-backward asymmetry A_{FB} measures the relative excess of Ξ^- (Ξ^+) baryons with p_z in the p (\bar{p}) direction. The asymmetry A_{NS} is given by the relative excess of the sum of Ξ^- and Ξ^+ baryons with p_z in the \bar{p} beam direction (north) with respect to the p beam direction (south). The asymmetry A_Ξ is the relative excess of negatively charged over positively charged baryons.

The initial $p\bar{p}$ state is invariant with respect to CP conjugation, which changes the sign of A_{NS} and A_Ξ , while A_{FB} remains unchanged. A non-zero value of A_{NS} or A_Ξ would indicate CP violation.

The asymmetry A'_{NS} is mainly due to differences in the product of the acceptance and efficiency between the northern hemisphere of the DØ detector with respect to the southern hemisphere. The difference in reconstruction efficiencies of Ξ^- and Ξ^+ baryons caused by the different inelastic interaction cross-sections of p and \bar{p} with the detector material creates the additional asymmetry A'_Ξ [1].

The raw asymmetries including terms up to second-order in the asymmetries are given by

$$\begin{aligned} A'_{\text{FB}} &= A'_{\text{NS}} A'_\Xi \\ &+ \frac{N_F(\Xi^-) - N_B(\Xi^-) + N_F(\Xi^+) - N_B(\Xi^+)}{N_F(\Xi^-) + N_B(\Xi^-) + N_F(\Xi^+) + N_B(\Xi^+)}, \end{aligned} \quad (3)$$

$$\begin{aligned} A'_{\text{NS}} &= A'_{\text{FB}} A'_\Xi \\ &+ \frac{-N_F(\Xi^-) + N_B(\Xi^-) + N_F(\Xi^+) - N_B(\Xi^+)}{N_F(\Xi^-) + N_B(\Xi^-) + N_F(\Xi^+) + N_B(\Xi^+)}, \end{aligned} \quad (4)$$

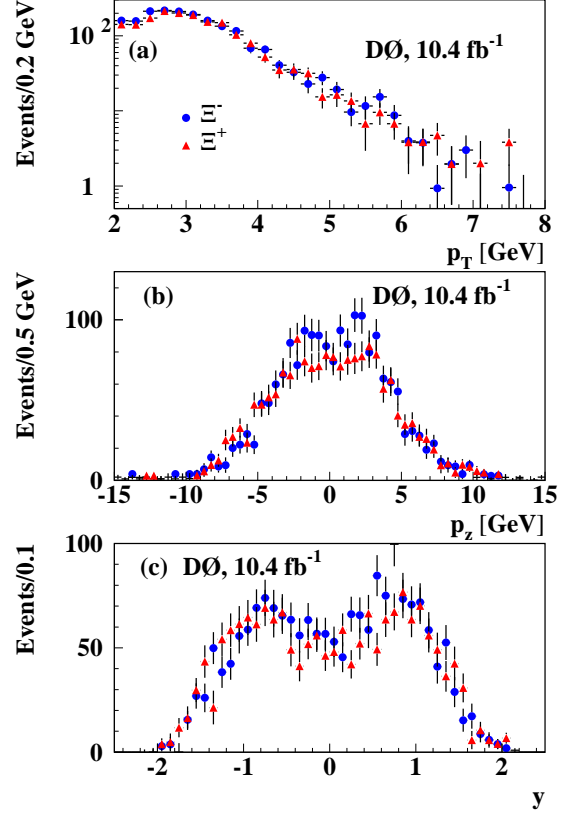


FIG. 3: Distributions of p_T , p_z , and y of reconstructed Ξ^- (circles) and Ξ^+ candidates (triangles) with $p_T > 2$ GeV, for the minimum bias data sample $p\bar{p} \rightarrow \Xi^\mp X$.

$$\begin{aligned} A'_\Xi &= A'_{\text{FB}} A'_{\text{NS}} \\ &+ \frac{N_F(\Xi^-) + N_B(\Xi^-) - N_F(\Xi^+) - N_B(\Xi^+)}{N_F(\Xi^-) + N_B(\Xi^-) + N_F(\Xi^+) + N_B(\Xi^+)}. \end{aligned} \quad (5)$$

The polarities of the solenoid and toroid magnets were reversed about once every two weeks during data-taking to collect approximately the same number of events for each of the four solenoid-toroid polarity combinations. We apply weights to equalize the sums of Ξ^- and Ξ^+ candidates reconstructed for each of the four polarity combinations. This averaging over magnet polarities cancels contributions from the detector geometry to A'_{FB} and A'_Ξ , but not to A'_{NS} [1].

The raw asymmetry A'_{FB} has negligible contributions from detector effects after averaging over solenoid and toroid magnet polarities. The raw asymmetries A'_{NS} and A'_Ξ are dominated by detector effects [1]. The quadratic term $A'_{\text{NS}} A'_\Xi$ in Eq. (3) corrects A'_{FB} for the detector effects A'_{NS} and A'_Ξ on the particle counts $N_F(\Xi^\mp)$ and $N_B(\Xi^\mp)$. We can therefore set $A'_{\text{FB}} = A_{\text{FB}}$ where A_{FB} is defined in Eq. (1).

TABLE I: Forward-backward asymmetry A_{FB} of Ξ^\mp baryons with $p_T > 2$ GeV in minimum bias events, $p\bar{p} \rightarrow \Xi^\mp X$, and muon events $p\bar{p} \rightarrow \mu\Xi^\mp X$, and A_{FB} of Ω^- and Ω^+ baryons with $p_T > 2$ GeV in muon events $p\bar{p} \rightarrow \mu\Omega^\mp X$. The first uncertainty is statistical, the second is systematic due to the detector asymmetry $A'_{\text{NS}}A'_\Xi$.

$ y $	$A_{\text{FB}} \times 100$ (Ξ^\mp , min. bias)	$A_{\text{FB}} \times 100$ (Ξ^\mp , with μ)	$A_{\text{FB}} \times 100$ (Ω^\mp , with μ)
0.0 to 0.5	$-2.78 \pm 3.20 \pm 0.34$	$-0.20 \pm 0.72 \pm 0.01$	$-3.43 \pm 2.90 \pm 0.13$
0.5 to 1.0	$5.23 \pm 2.85 \pm 0.55$	$-0.13 \pm 0.66 \pm 0.03$	$3.25 \pm 2.78 \pm 0.10$
1.0 to 1.5	$2.61 \pm 3.75 \pm 0.45$	$1.55 \pm 0.77 \pm 0.05$	$0.46 \pm 3.52 \pm 0.14$
1.5 to 2.0	$5.09 \pm 9.00 \pm 1.64$	$-1.14 \pm 2.05 \pm 0.27$	$5.75 \pm 10.86 \pm 5.70$

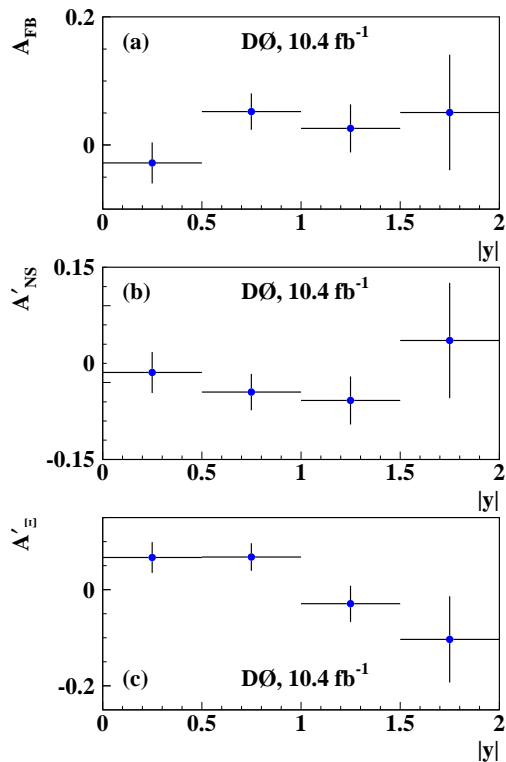


FIG. 4: Asymmetries $A'_{\text{FB}} = A_{\text{FB}}$, A'_{NS} and A'_Ξ of reconstructed Ξ^- and Ξ^+ candidates with $p_T > 2$ GeV, as a function of $|y|$, for the minimum bias data sample $p\bar{p} \rightarrow \Xi^\mp X$. The uncertainties are statistical.

MINIMUM BIAS SAMPLE EVENTS $p\bar{p} \rightarrow \Xi^\mp X$

The minimum bias sample contains 3.7×10^3 reconstructed Ξ^\mp candidates with $p_T > 2$ GeV. Distributions of p_T , p_z , and y for the Ξ^\mp candidates are shown in Fig. 3 and the corresponding raw asymmetries $A'_{\text{FB}} = A_{\text{FB}}$, A'_{NS} and A'_Ξ in Fig. 4. These asymmetries are calculated using Eqs. 3-5, neglecting the quadratic terms since they are small compared to the statistical uncertainties. The correction $A'_{\text{NS}}A'_\Xi$ needed to obtain $A'_{\text{FB}} = A_{\text{FB}}$ is measured to be consistent with zero within statistical uncertainties, see Figs. 4 (b) and (c). Thus, we choose not to apply this correction, but rather take the full mea-

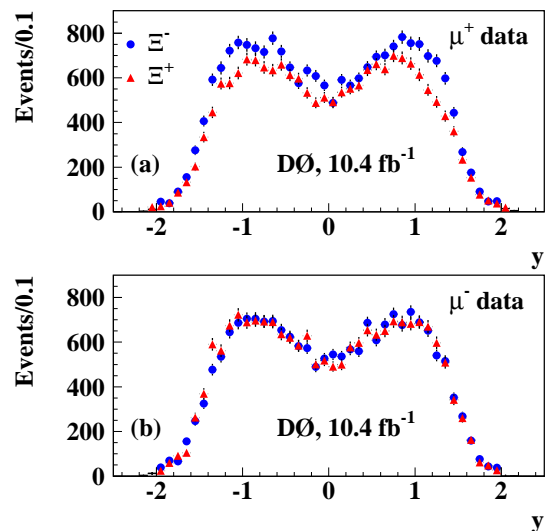


FIG. 5: Distributions of rapidity y for reconstructed Ξ^- (circles) and Ξ^+ candidates (triangles) in events with a (a) positively or (b) negatively charged muon for Ξ^\mp candidates with $p_T > 2$ GeV.

sured detector asymmetry $A'_{\text{NS}}A'_\Xi$ as the systematic uncertainty on the measurement of A_{FB} . The results are summarized in Table I.

MUON SAMPLE EVENTS $p\bar{p} \rightarrow \mu\Xi^\mp X$ AND $p\bar{p} \rightarrow \mu\Omega^\mp X$

To study the asymmetries using a larger data set, we consider $p\bar{p} \rightarrow \mu\Xi^\mp X$ and $p\bar{p} \rightarrow \mu\Omega^\mp X$ events taken from the single muon trigger sample. Charged particles with transverse momentum in the range $1.5 < p_T < 25$ GeV and $|\eta| < 2.2$ are considered as muon candidates. Muon candidates are further selected by matching central tracks with a segment reconstructed in the muon system and by applying tight quality requirements aimed at reducing false matching and background from cosmic rays and beam halo. To ensure that the muon candidate traverses the detector, including all three layers of the muon system, we require either $p_T > 4.2$ GeV or $|p_z| > 5.4$ GeV [8, 9]. The inclusive muon sample contains 2.2×10^9

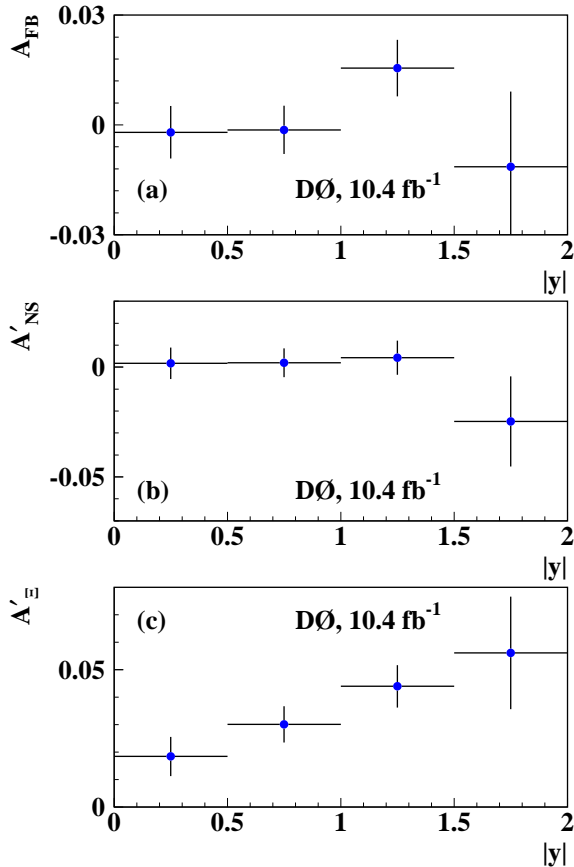


FIG. 6: Asymmetries $A'_{\text{FB}} = A_{\text{FB}}$, A'_{NS} and A'_{Ξ} of reconstructed Ξ^- and Ξ^+ candidates with $p_T > 2$ GeV, as a function of $|y|$, for $p\bar{p} \rightarrow \mu\Xi^{\mp}X$ events. The uncertainties are statistical.

reconstructed muons and 7.7×10^4 reconstructed Ξ^- and Ξ^+ candidates with $p_T > 2$ GeV, as well as 1.4×10^4 reconstructed Ω^- and Ω^+ candidates.

Rapidity distributions for reconstructed Ξ^- and Ξ^+ candidates are shown in Fig. 5. From these distributions we observe that (i) the detection efficiency for Ξ^- baryons is larger than for Ξ^+ baryons as explained above, and (ii) there are more $\Xi^{\mp}\mu^{\pm}$ than $\Xi^{\mp}\mu^{\mp}$ events. An example of a process with a correlated $\Xi^-\mu^+$ pair is the decay $\Xi_c^0 \rightarrow \Xi^-\mu^+X$. We find that the asymmetry A'_{FB} obtained with events containing a μ^+ is consistent with the corresponding asymmetry with μ^- within statistical uncertainties. We therefore combine the μ^+ and μ^- samples to obtain the asymmetries presented in Figs. 6 and 7.

The p_T , p_z , and y distributions for $p\bar{p} \rightarrow \mu\Omega^{\mp}X$ events are shown in Fig. 8, and the corresponding asymmetry A_{FB} is presented in Fig. 9. The Ξ^{\mp} and Ω^{\mp} asymmetries are summarized in Table I.

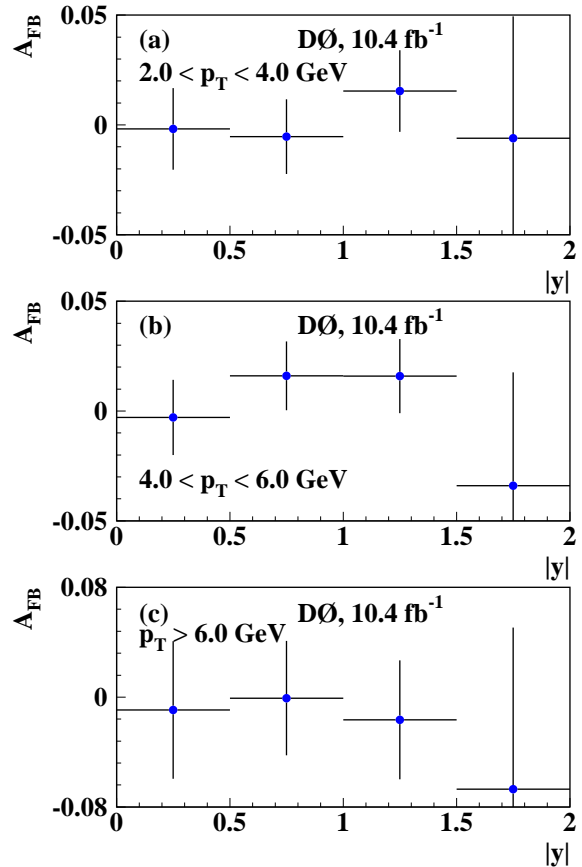


FIG. 7: Asymmetry $A'_{\text{FB}} = A_{\text{FB}}$ as a function of $|y|$ for $p\bar{p} \rightarrow \mu\Xi^{\mp}X$ events with (a) $2.0 < p_T < 4.0$ GeV, (b) $4.0 < p_T < 6.0$ GeV, and (c) $p_T > 6.0$ GeV. The uncertainties are statistical.

CONCLUSIONS

We have measured the forward-backward asymmetries A_{FB} in $p\bar{p} \rightarrow \Xi^{\mp}X$, $p\bar{p} \rightarrow \mu\Xi^{\mp}X$, and $p\bar{p} \rightarrow \mu\Omega^{\mp}X$ events using 10.4 fb^{-1} of integrated luminosity recorded with the D0 detector. We find that A_{FB} for Ξ^{\mp} and Ω^{\mp} are consistent with zero within uncertainties.

We thank the staffs at Fermilab and collaborating institutions, and acknowledge support from the Department of Energy and National Science Foundation (United States of America); Alternative Energies and Atomic Energy Commission and National Center for Scientific Research/National Institute of Nuclear and Particle Physics (France); Ministry of Education and Science of the Russian Federation, National Research Center ‘‘Kurchatov Institute’’ of the Russian Federation, and Russian Foundation for Basic Research (Russia); National Council for the Development of Science and Technology and Carlos Chagas Filho Foundation for the Support of Research in the State of Rio de Janeiro (Brazil); Department of

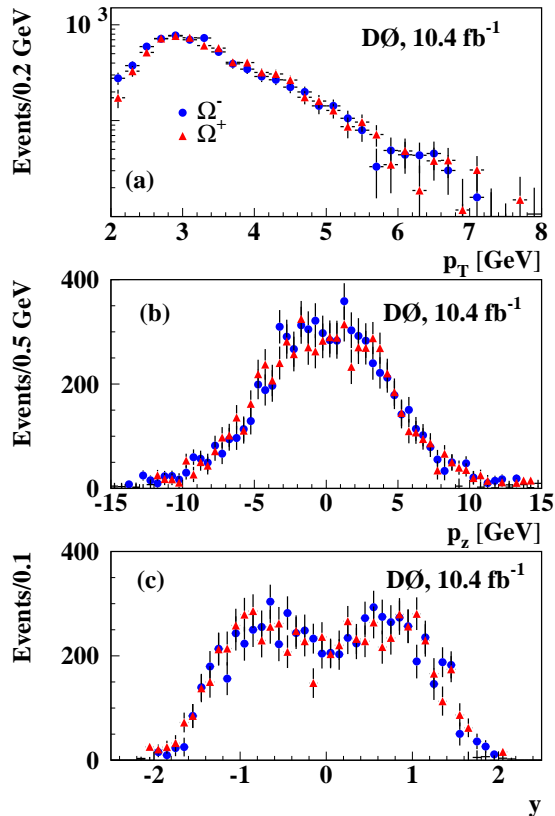


FIG. 8: Distributions of p_T , p_z , and y of reconstructed Ω^- (circles) and Ω^+ (triangles) with $p_T > 2$ GeV, for the data sample $p\bar{p} \rightarrow \mu\Omega^\mp X$.

Atomic Energy and Department of Science and Technology (India); Administrative Department of Science, Technology and Innovation (Colombia); National Council of Science and Technology (Mexico); National Research Foundation of Korea (Korea); Foundation for Fundamental Research on Matter (The Netherlands); Science and Technology Facilities Council and The Royal Society (United Kingdom); Ministry of Education, Youth and Sports (Czech Republic); Bundesministerium für Bildung und Forschung (Federal Ministry of Education and Research) and Deutsche Forschungsgemeinschaft (German Research Foundation) (Germany); Science Foundation Ireland (Ireland); Swedish Research Council (Sweden); China Academy of Sciences and National Natural Science Foundation of China (China); and Ministry of Education and Science of Ukraine (Ukraine).

[1] V.M. Abazov *et al.* (D0 Collaboration), Measurement of the forward-backward asymmetry of Λ and $\bar{\Lambda}$ production

in $p\bar{p}$ collisions, Phys. Rev. D **93**, 032002 (2016).

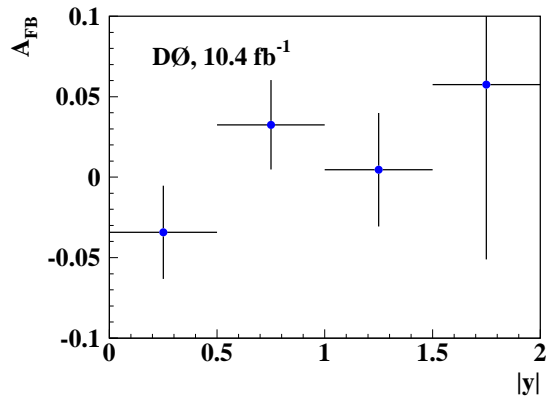


FIG. 9: Asymmetry A_{FB} as a function of $|y|$ for events $p\bar{p} \rightarrow \mu\Omega^\mp X$ for $p_T > 2$ GeV. The uncertainties are statistical.

- [2] V.M. Abazov *et al.* (D0 Collaboration), Measurement of the Forward-Backward Asymmetry in the Production of B^\pm in $p\bar{p}$ Collisions at $\sqrt{s} = 1.96$ TeV, Phys. Rev. Lett. **114**, 051803 (2015).
- [3] V.M. Abazov *et al.* (D0 Collaboration), Measurement of the forward-backward asymmetry in Λ_b^0 and $\bar{\Lambda}_b^0$ baryon production in $p\bar{p}$ collisions at $\sqrt{s} = 1.96$ TeV, Phys. Rev. D **91**, 072008 (2015).
- [4] V.M. Abazov *et al.* (D0 Collaboration), The upgraded D0 detector, Nucl. Instrum. Methods in Phys. Res. A **565**, 463 (2006).
- [5] V.M. Abazov *et al.* (D0 Collaboration), The muon system of the Run II D0 detector, Nucl. Instrum. Methods in Phys. Res. A **552**, 372 (2005).
- [6] S.N. Ahmed *et al.*, The D0 Silicon Microstrip Tracker, Nucl. Instrum. Methods Phys. Res. A **634**, 8 (2011).
- [7] R. Angstadt *et al.*, The layer 0 inner silicon detector of the D0 experiment, Nucl. Instrum. Methods Phys. Res. A **622**, 298 (2010).
- [8] V.M. Abazov *et al.* (D0 Collaboration), Measurement of the anomalous like-sign dimuon charge asymmetry with 9 fb $^{-1}$ of $p\bar{p}$ collisions, Phys. Rev. D **84**, 052007 (2011).
- [9] V.M. Abazov *et al.* (D0 Collaboration), Study of CP-violating charge asymmetries of single muons and like-sign dimuons in $p\bar{p}$ collisions, Phys. Rev. D **89**, 012002 (2014).
- [10] The pseudorapidity is given by $\eta = -\ln[\tan(\theta/2)]$, where θ is the polar angle with respect to the proton beam direction